

TERM PROJECT 1D MHD

TREY W. JENSEN¹

(Dated: December 16, 2016)

1. MAGNETOHYDRODYNAMICS

Magnetohydrodynamics (MHD) is an extension of hydrodynamics, where, on top of normal fluid equations such as the continuity equation and Euler equation, electromagnetism is added as if threading each fluid element. The partial differential equation we solve is of the general elliptic form,

$$\frac{\partial U}{\partial t} + \frac{\partial F}{\partial x} = 0, \quad (1)$$

where U is a vector of conserved quantities, and F is the vector of fluxes of those conserved quantities. In an adiabatic one-dimensional hydrodynamic code, we have initial conserved quantities mass, momentum, and energy written as $U = (\rho, \rho v, E)^T$, where ρ is the density, v the one-dimensional velocity, and E is the energy (transpose to signify it as a vector quantity). We compute E through $E = \rho e + \frac{1}{2}\rho v^2$, where the specific internal energy is found through the equation of state $P = (\gamma - 1)\rho e$ (where γ is the adiabatic index of our “ideal” fluid). The three conserved quantities, ρ , ρv , E , have fluxes given by $F = (\rho v, \rho v^2 + P, (E + P)v)^T$. If we want to simulate charged particles (or fluids) we are neglecting all the possible electromagnetic contributions. To account for this, we utilize the differential forms of Maxwell’s equations and Ampère’s law, and substituting Ohm’s law and Lorentz force to replace terms of the electric field (with ideal approximations). More explicitly we solve the equations (following closely from Stone et al. (2008); units are such that the magnetic permeability $\mu = 1$),

$$\frac{\partial \rho}{\partial t} + \nabla \cdot (\rho v) = 0, \quad (\text{mass cons.})$$

$$\frac{\partial \rho v}{\partial t} + \nabla \cdot (\rho v v - B B + P^*) = 0, \quad (\text{momentum cons.})$$

$$\frac{\partial E}{\partial t} + \nabla \cdot ((E + P^*)v - B(B \cdot v)) = 0, \quad (\text{energy cons.})$$

$$\frac{\partial B}{\partial t} - \nabla \times (v \times B) = 0, \quad (\text{Maxwell’s eq.})$$

where, in the case of one-dimension MHD, we have the conserved quantities and fluxes given by,

$$U = \begin{bmatrix} \rho \\ v_x \\ v_y \\ v_z \\ P \\ B_x \\ B_y \\ B_z \end{bmatrix}, \quad F = \begin{bmatrix} \rho v_x \\ \rho v_x^2 + P + B^2/2 - B_x^2 \\ \rho v_x v_y - B_x B_y \\ \rho v_x v_z - B_x B_z \\ (E + P^*)v_x - (B \cdot v)B_x \\ 0 \\ B_y v_x - B_x v_y \\ B_z v_x - B_x v_z \end{bmatrix},$$

where B is the magnetic field, $P^* = P + B^2/2$ is the total pressure, and here the total energy density is given by,

$$E = \frac{P}{\gamma - 1} + \frac{1}{2}\rho v^2 + \frac{B^2}{2}.$$

1.1. Computational Methods

To solve for the MHD equations in Section 1 requires solving for both a time step and spacial step. For the time progression, we implement a third-order Runge-Kutta scheme combined with forward Euler, given by,

$$U^{(1)} = U^n + \Delta t L(U^n),$$

$$U^{(2)} = \frac{3}{4}U^n + \frac{1}{4}U^{(1)} + \frac{1}{4}\Delta t L(U^{(1)}),$$

$$U^{n+1} = \frac{1}{3}U^n + \frac{2}{3}U^{(2)} + \frac{2}{3}\Delta t L(U^{(2)}),$$

where n signifies the n -th time step, and $L(U)$ is given by,

$$L(U) = -\frac{F_{i+1/2} - F_{i-1/2}}{\Delta x}.$$

We discretize our fluid into spacial cells that receive flux from the neighboring cells. We center our coordinates in the center of these cells, thus $i + 1/2$ ($i - 1/2$) would be the right (left) interface of the i -th cell. There are discontinuities at each interface (obviously from the discretization) that require a Riemann solver. In this case we use the Harten, Lax, van Leer (HLL) Riemann solver given by,

$$F^{HLL} = \frac{\alpha^+ F^L + \alpha^- F^R - \alpha^+ \alpha^- (U^R - U^L)}{\alpha^+ + \alpha^-},$$

where α^\pm are found from the minimal and maximal eigenvalues, λ , of the Jacobian of the conserved variables,

$$\lambda = (v_x - C_f, v_x - C_A, v_x - C_s, v_x + C_s, v_x + C_A, v_x + C_f)$$

where $C_{f,s}$ are the fast and slow-magnetosonic wave speeds and C_A is the Alfvén wave speed (see Stone et al. (2008) for more details). For a higher-order method of space, we compute the slopes of the quantities *near* the interfaces and feed them into F^{HLL} , which feeds into $L(U)$. For example, the left side of the right interface of the i -th cell is found via,

$$c_{i+1/2}^L = c_i + \frac{1}{2} \times \text{minmod}(1.5(c_i - c_{i-1}), 0.5(c_{i+1} - c_{i-1}), 1.5(c_{i+1} - c_i)),$$

where c is the input initial condition parameters (or, namely, conserved quantities), and the function minmod ensures that we do not accidentally “overshoot” the approximation causing inaccurate quantity differentials.

TJ796@nyu.edu

¹ Department of Physics, New York University, New York, NY 10003, USA

We can see that this requires two neighboring cells on either side of the computed interface, implying that we need two *ghost* cells on the left for the first cell, and on the right for the last cell. We use a Dirichlet boundary condition, where we simply fix the *ghost* cells as the initial conditions. Ultimately, using these newly computed conserved quantities from the higher-order spacial scheme ensures our interface flux is more accurately represented.

2. VALIDITY AND EXECUTION

A famous test is the Brio & Wu MHD Shock Tube Test problem. The initial conditions are step functions centered at $x_0 = 0.5$ with,

$$\begin{bmatrix} \rho \\ v_x \\ v_y \\ v_z \\ P \\ B_x \\ B_y \\ B_z \end{bmatrix} \text{ (Left)} = \begin{bmatrix} 1 \\ 0 \\ 0 \\ 0 \\ 1 \\ 0.75 \\ 1 \\ 0 \end{bmatrix}, \quad \& \quad \begin{bmatrix} \rho \\ v_x \\ v_y \\ v_z \\ P \\ B_x \\ B_y \\ B_z \end{bmatrix} \text{ (Right)} = \begin{bmatrix} 0.125 \\ 0 \\ 0 \\ 0 \\ 0.1 \\ 0.75 \\ -1 \\ 0 \end{bmatrix}, \quad (2)$$

and $\gamma = 2$. The results of running these initial conditions to $t_f = 0.12$ are shown in Figure 1, and qualitatively agree well with what is in the literature (see <https://astro.uni-bonn.de/~jmackey/jmac/node7.html> for example). This test reveals proper propagation of waves, including the compound waves, rarefactions, contact discontinuities, and shocks. For a more quantitative approach of validity, we introduce isentropic initial conditions that, by physical design, maintain entropy. The initial conditions were given by,

$$\begin{aligned} \rho(x) &= \rho_0(1 + \alpha f(x)) \\ P(x) &= P_0 \left(\frac{\rho(x)}{\rho_0} \right)^\gamma \\ B_y(x) &= (1 + \alpha f(x)) \end{aligned} \quad (3)$$

where $\rho_0 = 1, P_0 = 1, \alpha = 0.2, \gamma = 5/3$, and $f(x)$ is a $1-\sigma$ gaussian perturbation centered on $x_0 = 2$ with $\sigma = 0.4$, where everything outside of $|x - x_0| < \sigma$ is zero. We can see the outcome of the simulation at $t_f = 1$ (and intermediate intervals) in Figure 2. To check if our simulation obeys theoretical physical prediction, we computed how the integrated L_1 error in entropy (i.e. $|s_0 - s_f|$) scales with the number of steps N . We see a slope of convergence $L_1 \propto N^m$ with $m \approx -2.57$ which implies this was

higher than a second-order result. This problem is well-behaved for short time periods with no discontinuities or jumps, so convergence is also well-behaved. Finally, we tested the consequences of perturbing a uniform, equilibrium fluid with a gaussian magnetic field (B_y identical to that in Eq. 3). Here we generated a movie that can be seen at <https://youtu.be/JJbPpWo2wpA>. This simulation ultimately reveals the consequences of Alfvén waves. The initial magnetic field in the y direction wants to repel, and initially splits into two Alfvén waves, but in order to do this, it drags the material with it leaving a void of density at the initial perturbation. This void would normally be filled in, but because of the magnetic field also battling movement of fluid, it creates a self-sustained void in pressure and density, trapping the surplus magnetic field at the center. The two Alfvén waves propagate indefinitely dragging fluid with it.

3. FUTURE WORK

The original inspiration for this work was to model the galactic magnetic field of the Milky Way galaxy. Unfortunately that requires a three-dimensional algorithm and is the scale of a Ph.D. thesis. More specifically, the next steps would be to try to extend this to spherical coordinates and impose sheering velocities from the gravitational potential such as a black hole, to ultimately, given an initial magnetic field of poloidal geometry, see how this initial field alters. Along with this, implementing striated random fields within the disk to mimic super novae within the galaxy or the like as mentioned in Jansson & Farrar (2012). These goals require a supercomputer, and are, of course, over-ambitious in nature for a project such as this.

I would like to thank Professor MacFadyen for the intricate and well organized lectures that gave way to even learning Python from scratch, and supplied resources to dabble near the frontier of research regarding computational physics. And especially to Geoff, who put up with an impossible amount of shit from all students, me included. I would go postal having to pore through amateurish (again, I am not excluded) programs. Thank you.

REFERENCES

- Jansson R., Farrar G. R., 2012, ApJ, 757, 14
- Stone J. M., Gardiner T. A., Teuben P., Hawley J. F., Simon J. B., 2008, ApJS, 178, 137

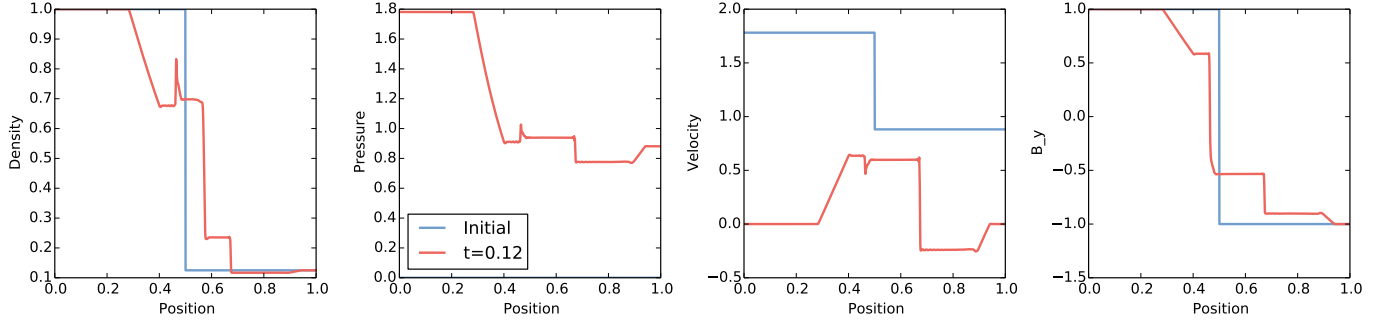


Figure 1. Plot of the density, pressure, velocity in the x -direction, and magnetic field in the y -direction. The initial conditions are given in Eq. 2. The simulation ran until $t = .12$. This is for $N = 1000$ spatial grid cells. The units are arbitrary.

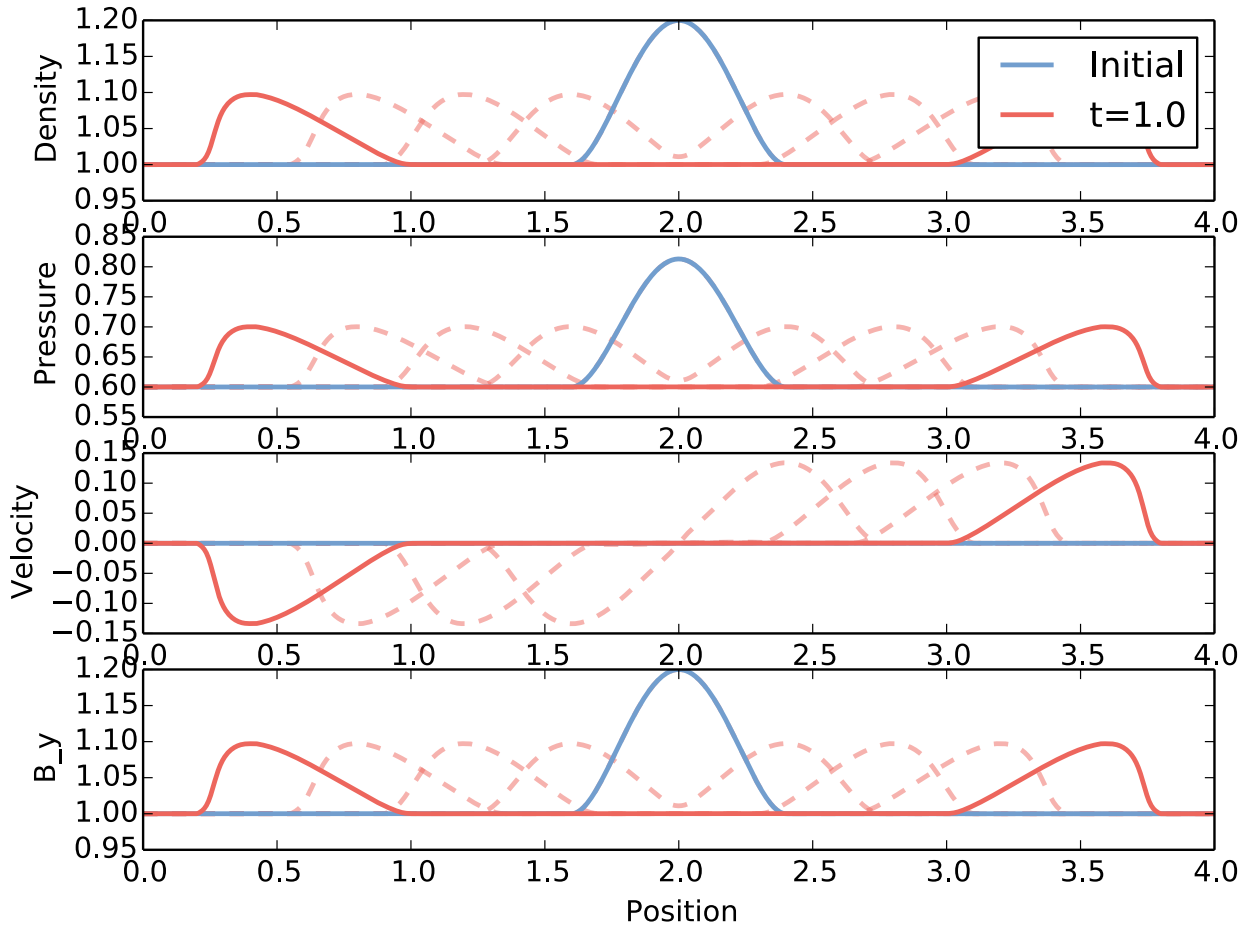


Figure 2. Plot of the density, pressure, velocity in the x -direction, and magnetic field in the y -direction. The initial conditions are given in Eq. 3. The semitransparent lines are intermediate time steps. This is for $N = 1000$ spatial grid cells. The units are arbitrary.

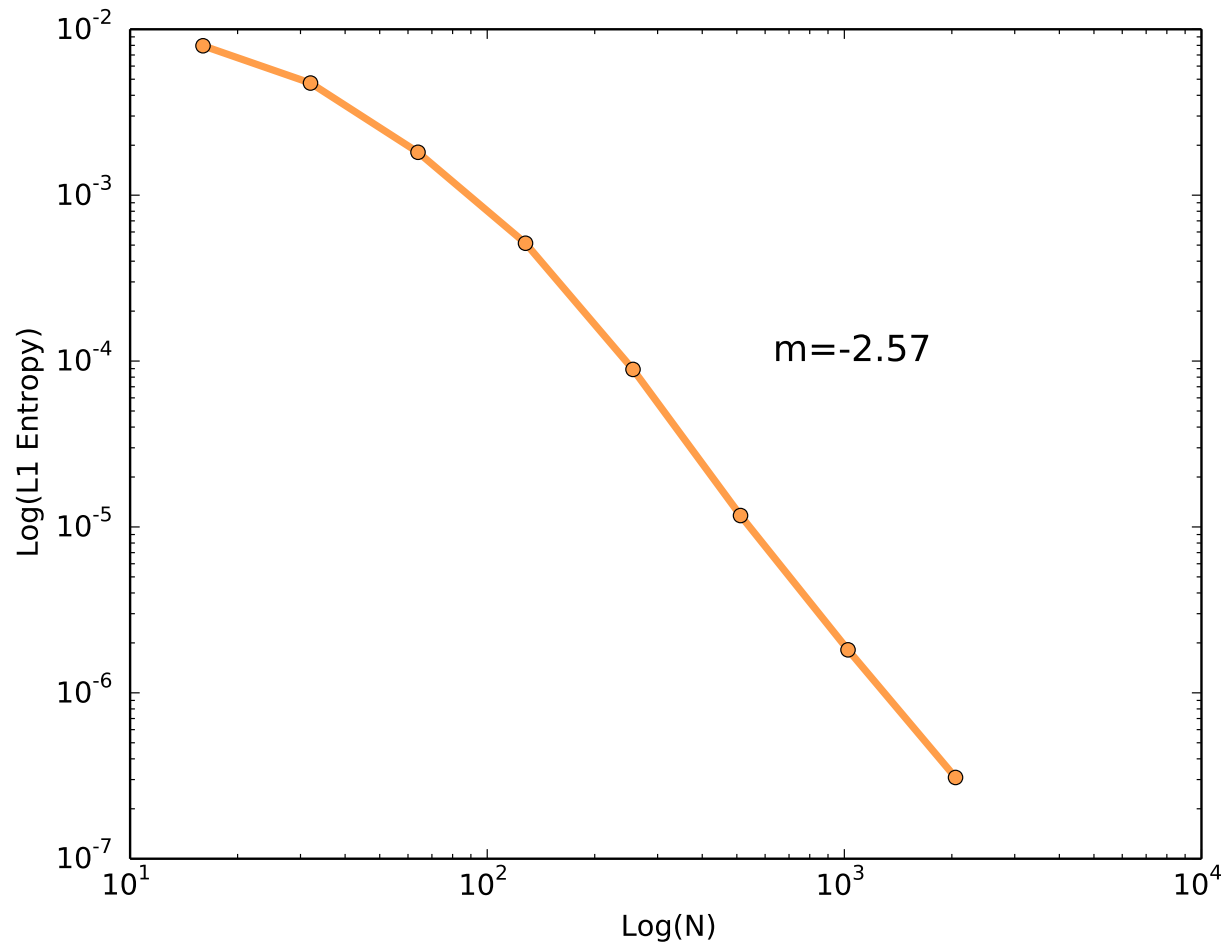


Figure 3. Log-Log plot of the convergence of iterating the simulation of initial conditions given by Eq. 3 with different number of spacial grid cells, N . The slope of convergence, m , is reported.